Data in Brief 31 (2020) 105870

Contents lists available at ScienceDirect

Data in Brief

journal homepage: www.elsevier.com/locate/dib

Data Article

2D and 3D graphical datasets for bamboo-inspired tubular scaffolds with functional gradients: micrographs and tomograms

Kaiyang Yin[a], Max D. Mylo[b,c], Thomas Speck[b,c], Ulrike G.K. Wegst[a,d,*]

[a] Thayer School of Engineering, Dartmouth College, Hanover, NH 03755, USA
[b] Plant Biomechanics Group, Botanic Garden, University of Freiburg, Freiburg, Germany
[c] Cluster of Excellence livMatS @ FIT – Freiburg Center for Interactive Materials and Bioinspired Technologies, Freiburg, Germany
[d] Department of Physics, Northeastern University, Boston, MA 02115, USA

ARTICLE INFO

Article history:
Received 11 May 2020
Revised 26 May 2020
Accepted 8 June 2020
Available online 17 June 2020

Keywords:
Coaxial Freeze Casting
Spray Coating
Brush Coating
Bending
Microtomography

ABSTRACT

Presented in this article are 2D and 3D graphical datasets in the form of micrographs and tomograms that were obtained as part of a systematic microstructural characterization by scanning electron microscopy and X-ray microtomography to illustrate freeze-cast bamboo-inspired tubular scaffolds with functional gradients ("Bamboo-inspired Tubular Scaffolds with Functional Gradients" [1]). Four material combinations of the coaxial 'core-shell' molds and their two end pieces were used to freeze cast highly porous tubes (Tube/Rod/Holder): ASA (Aluminum, 316 Stainless Steel, Aluminum), ASP (Aluminum, 316 Stainless Steel, Epoxy (Plastic)), SCA (316 Stainless Steel, Copper, Aluminum), and CSP (Copper, 316 Stainless Steel, Epoxy (Plastic)). Three techniques were used to coat the best performing CSP freeze-cast tubes: spray freezing (SF), spray coating (SC), and brush freezing (BF). The structure and density profile of the uncoated and coated tubes was quantified using X-ray microtomography and their functional gradients, and the resulting

DOI of original article: 10.1016/j.jmbbm.2020.103826
* Corresponding author.
E-mail address: u.wegst@northeastern.edu (U.G.K. Wegst).

https://doi.org/10.1016/j.dib.2020.105870

mechanical performance in bending were determined and compared. The structure-property-processing correlations determined for the coated and uncoated coaxially freeze cast tubular scaffolds offer strategies for the biomimetic design of bamboo-inspired porous tubes, which emulate bamboo's stiff outer shell supported by a porous, elastic inner layer to delay the onset of ovalization and failure, thereby increasing the tubes' mechanical efficiency.

Specifications Table

Subject	Materials Science
Specific subject area	Biomaterials, Biomimetic Materials
Type of data	Tables, Figures, Videos
How data were acquired	Scanning Electron Microscopy (Vega 3, Tescan, Brno, Czech Republic); X-ray Microtomography (Skyscan 1272, Bruker, Kontich, Belgium: 50 kV, 360° scans, 1.5 µm pixel resolution; NRecon Reconstruction Software)
Data format	Raw and Analyzed Data Files.
Parameters for data collection	Highly porous freeze-cast tubes were imaged in their dry state after lyophilization, either complete (X-ray microtomography) or after longitudinal and transverse sectioning (scanning electron microscopy.
Description of data collection	Scanning electron micrographs and the static and dynamic volume renderings of the X-ray microtomograms illustrate the tubes' microstructures in 2D and 3D, respectively.
Data source location	Provided with this Data article as Supplementary Files
Data accessibility	With the Article
Related research article	Kaiyang Yin, Max D. Mylo, Thomas Speck, Ulrike G.K. Wegst (2020) Bamboo-inspired Tubular Scaffolds with Functional Gradients, J. Mech. Behav. Biomed. Mater. https://doi.org/10.1016/j.jmbbm.2020.103826

Value of the data

- The combination of SEM micrographs with X-ray microtomograms illustrate particularly well how different mold designs and coating techniques result in hierarchical microstructures and graded pore morphologies along the length and across the section of radially freeze-cast tubes.
- The systematic correlations between structure and processing parameters discovered in this study benefit the freeze casting community with strategies for the custom-design of graded tubes and the biomedical community, who may wish to use them, for example, as conduits for peripheral nerve repair or as soft ureteral stents.
- The comprehensive data presented for functionally-graded bamboo-inspired tubes along the length and across the section can serve as a benchmark for tubes made with modified processing conditions or different fabrication techniques.

1. Data Description

1.1. Tube Microstructures by Scanning Electron Microscopy and X-ray Microtomograhy

Presented in Figs. 1-8 are the results of a systematic microstructural characterization of freeze-cast [11–15] bamboo-inspired [1–6] tubular scaffolds [1,7–10] with functional gradients. Shown are scanning electron micrographs (Fig. 1) and volume renderings of X-ray microtomo-

Fig. 1. Longitudinal sections of SCA, ASP, CSP, and ASA tubes.

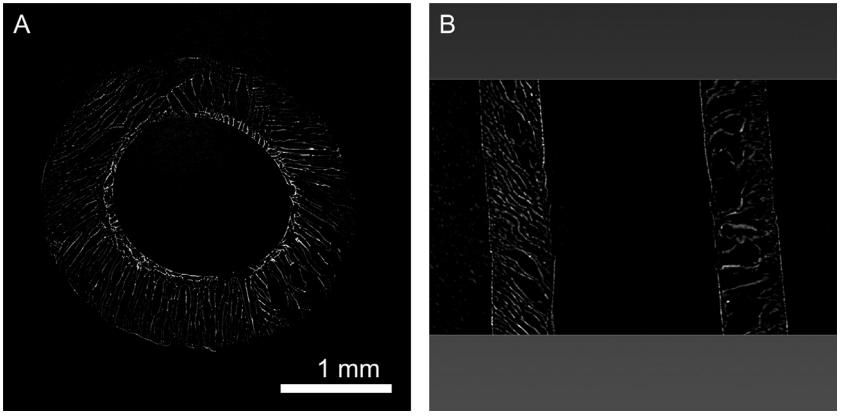

Fig. 2. Transverse (left) and longitudinal (right) sections of a typical ASA tube.

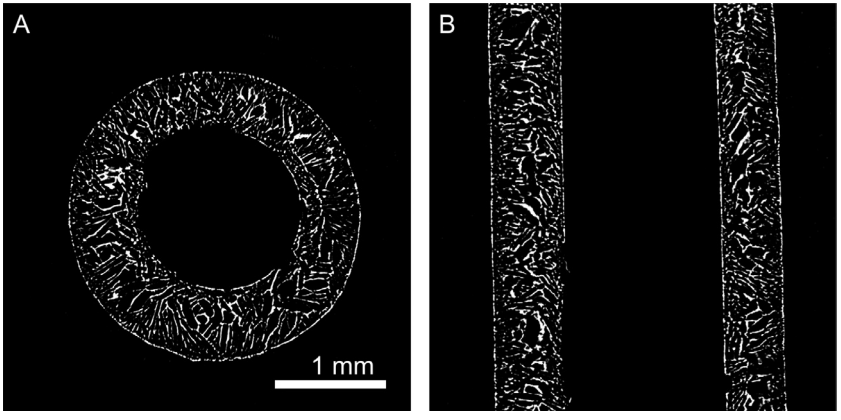

Fig. 3. Transverse (left) and longitudinal (right) sections of a typical ASP tube.

Table 1
Material combinations of the coaxial 'core-shell' molds and their two end pieces [1].

Abbreviation	Tube	Rod	Holder
ASA	Aluminum	316 Stainless Steel	Aluminum
ASP	Aluminum	316 Stainless Steel	Epoxy (Plastic)
SCA	316 Stainless Steel	Copper	Aluminum
CSP	Copper	316 Stainless Steel	Epoxy (Plastic)

grams (Figs. 2-8). Four material combinations were used for the manufacture of the coaxial 'core-shell' freeze-casting molds and the two end pieces that seal them; the materials are listed in the sequence Tube-Rod-Holder [1,7–10]. The scanning electron micrographs of longitudinal sections of highly porous freeze cast tubes shown in Fig. 1 were made with following Tube-Rod-Holder combinations (Table 1): SCA (316 Stainless Steel, Copper, Aluminum), ASP (Aluminum, 316 Stainless Steel, Epoxy (Plastic)), CSP (Copper, 316 Stainless Steel, Epoxy (Plastic)), ASA (Aluminum, 316 Stainless Steel, Aluminum) [1].

Figs. 2-8 show A) transverse and B) longitudinal sections through volume renderings of X-ray tomograms of freeze-cast ASA, ASP, CSP, and SCA tubes, and CSP tubes coated by brush freezing (BF), spray coating (SC), and spray freezing (SF) [1].

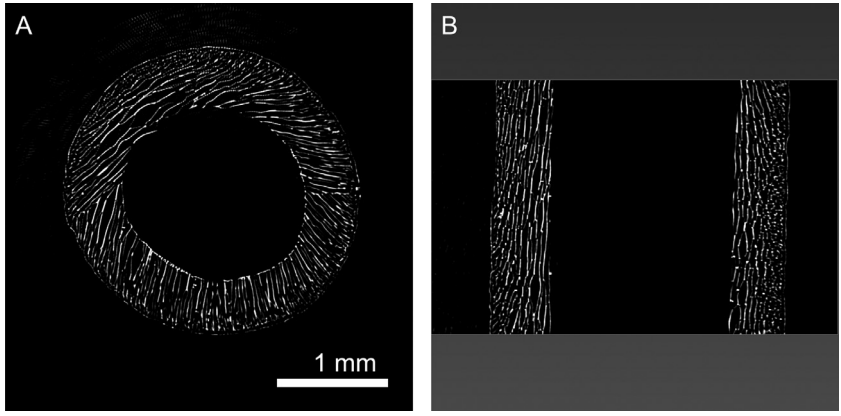

Fig. 4. Transverse (left) and longitudinal (right) sections of a typical CSP tube.

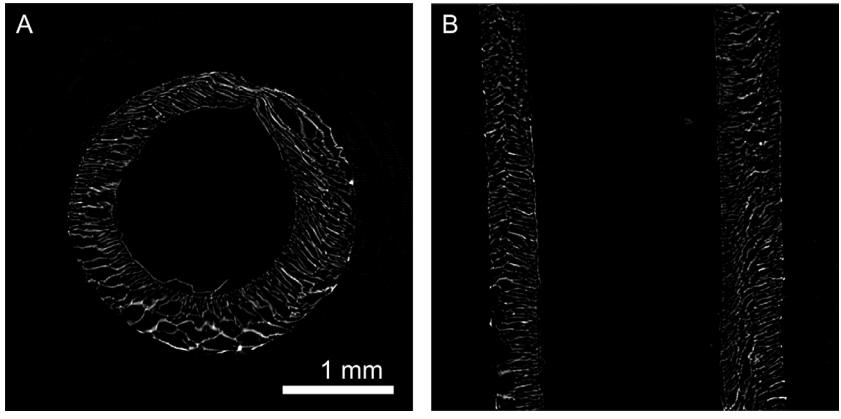

Fig. 5. Transverse (left) and longitudinal (right) sections of a typical SCA tube.

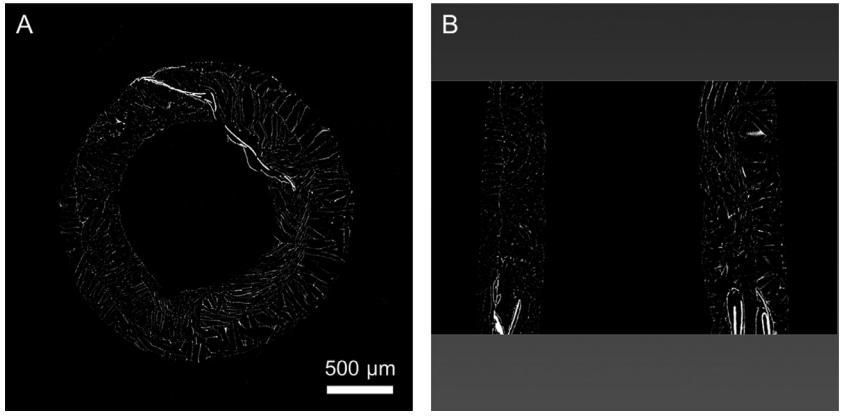

Fig. 6. Transverse (left) and longitudinal (right) sections of a typical BF-CSP tube.

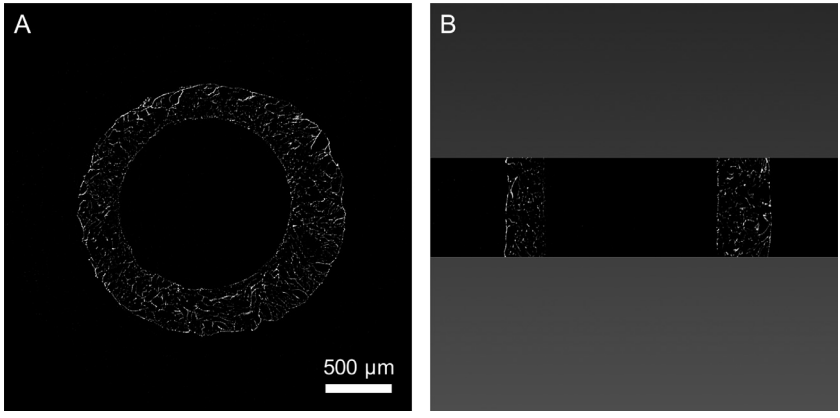

Fig. 7. Transverse (left) and longitudinal (right) sections of a typical SC-CSP tube.

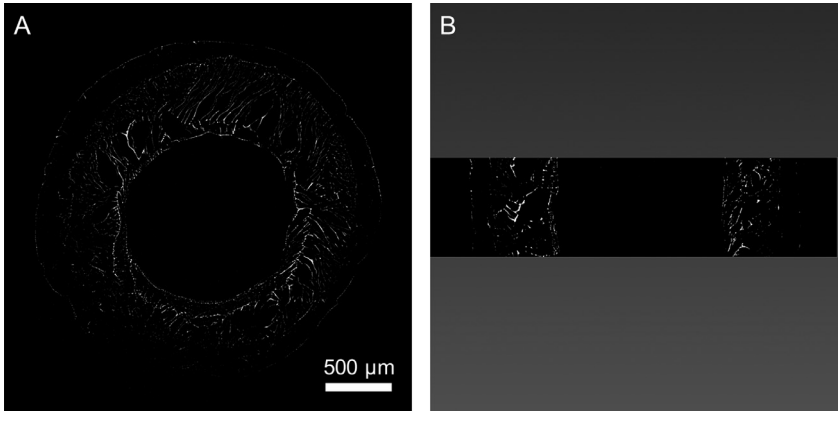

Fig. 8. Transverse (left) and longitudinal (right) sections of a typical SF-CSP tube.

1.2. Volume Renderings of X-ray Microtomograms

Shown in Videos 1-7 are 360° rotation loops of the volume renderings of X-ray microtomograms of freeze-cast ASA, ASP, CSP, and SCA tubes, and BF-, SC-, and SF coated CSP tubes.

2. Experimental Design, Materials, and Methods

2.1. Chitosan Solution Preparation

The chitosan solution for freeze casting and brush freezing was prepared by mixing 3.5% w/v chitosan (Chitoceuticals Chitosan 95/200, Heppe Medical Chitosan GmbH, Germany) in 1.5% v/v acetic acid (ACS grade, EMD Millipore, MA, USA) solution on the roller mixer (Wheaton, NJ, USA) for 24 hours. The chitosan solution for spray coating and spray freezing was 1.2% w/v in 1% v/v acetic acid, prepared by the same method. This composition was chosen because it is particularly well suited for spray coating. Decreasing the concentration would cause the droplets to freeze before reaching and attaching to the tube; increasing it would result in too viscous a solution for the formation of a homogeneous mist, instead the solution would drip from the

nozzle. The fluorescein stained chitosan was prepared by staining chitosan flakes in 0.05 mg/mL fluorescein sodium salt (Sigma-Aldrich, MO, USA) and 0.05M 1-Ethyl-3-(3-dimethylaminopropyl-carbodiimide) (EDC, Sigma-Aldrich, MO, USA) in phosphate buffered saline (PBS, VWR, PA, USA) solution for 6 hours, and washing in DI water for 12 hours [8]. The stained chitosan solutions (1.2% w/v and 3.5% w/v) were prepared using the same procedure, then stored in the dark.

2.2. Freeze Casting of Tubular Scaffolds

The mold for freeze casting was a coaxially fixed tube (3.0 mm inner diameter, 80 mm in length), rod (2 mm in diameter, 100 mm in length), and space holder combination of different materials (Table 1). The chitosan solution was injected into the gap between the tube and the rod, before the mold was placed in a -80°C freezer (HF-5017W-PA, VWR, PA, USA) for 20 minutes. The frozen chitosan tubes were demolded and lyophilized at 0.008 mbar and a -85°C coil temperature in a lyophilizer (Freezone 6 Plus, Labconco, MO, USA) for 24 hours. The freeze-dried chitosan tubes were neutralized by 15 minutes immersion in 0.4% w/v sodium hydroxide (reagent grade, anhydrous, Sigma-Aldrich, MO, USA) in 95% ethanol (200 proof, Koptec, PA, USA), followed by 6 hours of washing in deionized water. The chitosan tubes were stained with 0.01% w/v direct red 23 (Sigma-Aldrich, MO, USA) in PBS solution for 12 hours in the dark, then washed three times in deionized water [16]. The stained and unstained tubes were either flash frozen and lyophilized for spray coating and mechanical testing, or stored in the wet state for spray freezing and brush freezing.

2.3. Spray Coating

The dry tubes were attached coaxially and horizontally to a spinning motor on the bed of a 3-axis stage. An atomizer nozzle (NS60K, Sonaer Inc., NY, USA) was attached to the moving head of the stage. The chitosan solution (1.2% w/v) was fed into the nozzle by a syringe pump (NE-300, New Era Pump Systems Inc., NY, USA) at a pumping rate of 10 mL/hour, and atomized at 60 kHz, 95% power. Spray coating of the 8 mm long tube was conducted by spinning the tube at 60 rpm, and nozzle motion rate of 1 mm/s along the axial direction of the tube for two round trips at a vertical distance of 10 mm from the tube. Finally, filtered air was blown onto the tube to ease the drying of the coating.

2.4. Spray Freezing

For spray freezing, a stainless-steel dwell pin (1.8 mm diameter) was gently drilled into the lumen of the frozen CSP tube replacing the ice core. The pin was attached to the same spraying system with a 15 mm thick layer of dry ice at 15 mm below the spinning axis. Chitosan solution (1.2% w/v) was fed at a rate of 40 mL/hour into the nozzle. Spray freezing was conducted at a spinning rate of 120 rpm, and nozzle motion rate of 1 mm/s for one round trip. The tubes were first acclimatized in the -80°C freezer, then lyophilized.

2.5. Brush Coating Followed by Freezing

A nylon artistic brush (size #0, Bomega) was attached to the stage instead of the atomizer nozzle. The brush was wet by the 3.5% w/v chitosan solution, and 0.25 mL chitosan solution was added onto both sides of the brush. Brush coating was conducted by spinning the tube at 120 rpm with a brush motion rate of 1 mm/s for two round trips. The tip of the brush was just in contact with the tube. Finally, the resulting tubes were transferred into a -80°C freezer and removed only once completely frozen, then lyophilized.

2.6. Structural Analysis Scanning Electron Microscopy

The tubes were sliced with a razor blade, mounted onto the sample stub, and sputter coated with roughly 10 nm gold (Hummer 6.2, Anatech, CA, USA), then imaged using a Vega 3 (Tescan, Brno, Czech Republic).

2.7. X-Ray Microtomography and Analysis

The microtomographic analysis of all scaffolds was conducted using a high-resolution 3D X-ray microscope (Bruker Skyscan 1272, Kontich, Belgium) with a pixel resolution of 1.5 μm, image dimensions of 2452 pixels $\times$ 1640 pixels, imaging the samples in a 360° scan with a rotation step size of 0.6°, a source voltage of 50 kV without filter, a source current of 200 μA, frame image averaging over 3 frames, and a random movement correction of 10. Data reconstruction was carried out using the NRecon software (Version 1.6.10.1, Skyscan, Kontich, Belgium) with smoothing set to 3 (using a Gaussian smoothing kernel of 2), and ring artefact and beam hardening corrections applied. The reconstructed data was visualized in Avizo (Version 9.1, Thermo Fisher, OR, USA).

2.8. Bending Tests

For guided, static three-point bending tests an apparatus was designed according to ASTM standard D790-17 (ASTM International, 2017) with a span of L = 45 mm. The radius of the upper and the lower loading noses was R = 5 mm. The samples were compressed using the Instron and BioPuls Bath system (33% r.h.) with 5 N load cell and at a strain rate of 0.01 min^{-1} (displacement rate 1.2 mm/min) until a maximum flexural strain of $\varepsilon_f = 5\%$ ($\delta = 6$ mm) was reached.

Declaration of Competing Interest

The authors declare that they have no known competing financial interests or personal relationships which have, or could be perceived to have, influenced the work reported in this article.

Acknowledgments

The authors would like to thank Kasidet “Jing” Trerayapiwat for the manufacture of the 3-point bending fixture. K.Y. and U.G.K.W. gratefully acknowledge financial support through NIH-NICHD Award R21HD087828, NSF-CMMI Award 1538094, and NASA Award 80NSSC18K0305. K.Y. and U.G.K.W. would like to thank the Shared Resources facilities (Electron Microscopy Facilities) at the Norris Cotton Cancer Center at Dartmouth College (NCI Cancer Center Support Grant 5P30 CA023108-37) and the Class of 1978 Life Science Center at Dartmouth College for imaging support. M.M. and T.S. are grateful for funding by the Deutsche Forschungsgemeinschaft (DFG, German Research Foundation) under Germany’s Excellence Strategy–EXC-2193/1–390951807. The content is solely the responsibility of the authors and does not necessarily represent the official views of the National Institutes of Health.

Supplementary materials

Supplementary material associated with this article can be found, in the online version, at doi:10.1016/j.dib.2020.105870.

References

[1] K. Yin, M.D. Mylo, T. Speck, U.G.K. Wegst, Bamboo-inspired Tubular Scaffolds with Functional Gradients, J. Mech. Behav. Biomed. Mater (2020), doi:10.1016/j.jmbbm.2020.103826.

[2] U.G.K. Wegst, M.F. Ashby, The structural efficiency of orthotropic stalks, stems and tubes, J. Mater. Sci. 42 (2007) 9005–9014, doi:10.1007/s10853-007-1936-8.

[3] U.G.K. Wegst, Bamboo and Wood in Musical Instruments, Annu. Rev. Mater. Res. 38 (2008) 323–349, doi:10.1146/annurev.matsci.38.060407.132459.

[4] U.G.K. Wegst, Bending efficiency through property gradients in bamboo, palm, and wood-based composites, J. Mech. Behav. Biomed. Mater. 4 (2011) 744–755, doi:10.1016/j.jmbbm.2011.02.013.

[5] Z. Liu, M.A. Meyers, Z. Zhang, R.O. Ritchie, Functional gradients and heterogeneities in biological materials: Design principles, functions, and bioinspired applications, Prog. Mater. Sci. 88 (2017) 467–498, doi:10.1016/j.pmatsci.2017.04.013.

[6] M. Sato, A. Inoue, H. Shima, Bamboo-inspired optimal design for functionally graded hollow cylinders, PLOS ONE 12 (2017) e0175029, doi:10.1371/journal.pone.0175029.

[7] K. Yin, P. Divakar, J. Hong, K.L. Moodie, J.M. Rosen, C.A. Sundback, M.K. Matthew, U.G.K. Wegst, Freeze-cast Porous Chitosan Conduit for Peripheral Nerve Repair, MRS Adv 3 (2018) 1677–1683, doi:10.1557/adv.2018.194.

[8] K. Yin, P. Divakar, U.G.K. Wegst, Freeze-casting porous chitosan ureteral stents for improved drainage, Acta Biomater 84 (2019) 231–241, doi:10.1016/j.actbio.2018.11.005.

[9] K. Yin, P. Divakar, U.G.K. Wegst, Plant-Derived Nanocellulose as Structural and Mechanical Reinforcement of Freeze-Cast Chitosan Scaffolds for Biomedical Applications, Biomacromolecules 20 (2019) 3733–3745, doi:10.1021/acs.biomac.9b00784.

[10] F.Y. Su, J.R. Mok, J. McKittrick, Radial-Concentric Freeze Casting Inspired by Porcupine Fish Spines, Ceramics 2 (2019) 161–179, doi:10.3390/ceramics2010015.

[11] U.G.K. Wegst, M. Schecter, A.E. Donius, P.M. Hunger, Biomaterials by freeze casting, Philos. Trans. R. Soc. A 368 (2010) 2099–2121, doi:10.1098/rsta.2010.0014.

[12] H. Bai, D. Wang, B. Delattre, W. Gao, J.D. Coninck, S. Li, A.P. Tomsia, Biomimetic gradient scaffold from ice-templating for self-seeding of cells with capillary effect, Acta Biomater 20 (2015) 113–119, doi:10.1016/j.actbio.2015.04.007.

[13] U.G.K. Wegst, H. Bai, E. Saiz, A.P. Tomsia, R.O. Ritchie, Bioinspired structural materials. Nat, Mater 14 (2015) 23–36, doi:10.1038/nmat4089.

[14] S. Mohan, I.C. Hernández, W. Wang, K. Yin, C.A. Sundback, U.G.K. Wegst, N. Jowett, Fluorescent Reporter Mice for Nerve Guidance Conduit Assessment: A High-Throughput in vivo Model, The Laryngoscope 128 (2018) E386–E392, doi:10.1002/lary.27439.

[15] B.A. Harley, A.Z. Hastings, I.V. Yannas, A. Sannino, Fabricating tubular scaffolds with a radial pore size gradient by a spinning technique, Biomaterials 27 (2006) 866–874, doi:10.1016/j.biomaterials.2005.07.012.

[16] C.T. Anderson, A. Carroll, L. Akhmetova, C. Somerville, Real-Time Imaging of Cellulose Reorientation during Cell Wall Expansion in Arabidopsis Roots, Plant Physiol 152 (2010) 787–796, doi:10.1104/pp.109.150128.